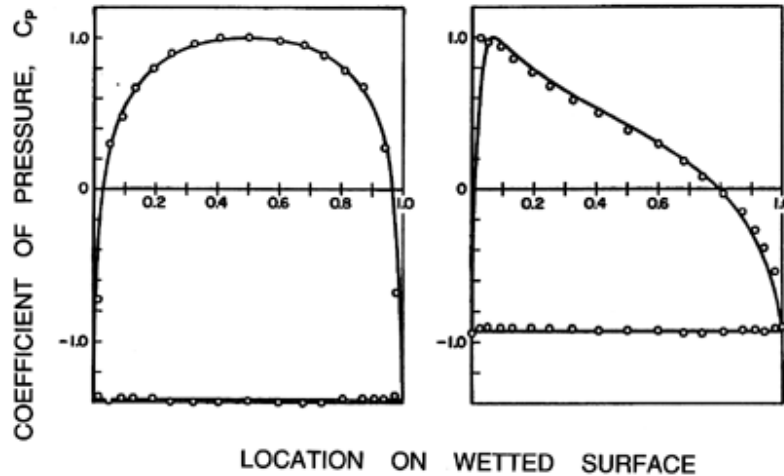# Some Nonlinear Results

Figure 1: Comparison of pressure distributions on the surface of a flat plate set at an angle, α, to the oncoming stream. The theory of Wu (1956, 1962) (solid lines) is compared with the measurements in wake flow made by Fage and Johansen (1927) ($\circ$). The case on the left is for a flat plate set normal to the stream ($\alpha = 90°$) and a wake coefficient of $\sigma = 1.38$; the case on the right is $\alpha = 29.85°$, $\sigma = 0.924$. Adapted from Wu (1962).

Wu (1956, 1962) (see also Mimura 1958) generated the solution for a flat plate at an arbitrary angle of incidence using the open-wake model and the methods described in the preceding section. The comparison between the predicted pressure distributions on the surface of the plate and those measured by Fage and Johansen (1927) in single phase, separated wake flow is excellent, as shown by the examples in Figure 1. Note that the effective cavitation number for the wake flow (or base pressure coefficient) is not an independent variable as it is with cavity flows. In Figure 1 the values of σ are taken from the experimental measurements. Data such as that presented in Figure 1 provides evidence that free streamline methods have value in wake flows as well as in cavity flows.

The lift and drag coefficients at various cavitation numbers and angles of incidence are compared with the experimental data of Parkin (1958) and Silberman (1959) in Figures 2 and 3. Data both for supercavitating and partially cavitating conditions are shown in these figures, the latter occurring at the higher cavitation numbers and lower incidence angles. The calculations tend to be quite unstable in the region of transition from the partially cavitating to the supercavitating state, and so the dashed lines in Figures 2 and 3 represent smoothed curves in this region. Later, in section (Nuh), we continue the discussion of this transition. For the present, note that the nonlinear theory yields values for the lift and the drag that are in good agreement with the experimental measurements. Wu and Wang (1964a) show similar good agreement for supercavitating, circular-arc hydrofoils.

The solution to the cavity flow of a flat plate set normal to an oncoming stream, $\alpha = 90°$, is frequently quoted (Birkhoff and Zarantonello 1957, Woods 1961), usually for the case of the Riabouchinsky model. At small cavitation numbers (large cavities) the asymptotic form of the drag coefficient, C_D, is (Wu 1972)

$$C_D(\sigma) = \frac{2\pi}{\pi + 4}\left[1 + \sigma + \frac{\sigma^2}{(8\pi + 32)} + O(\sigma^4)\right] \tag{Nuf1}$$
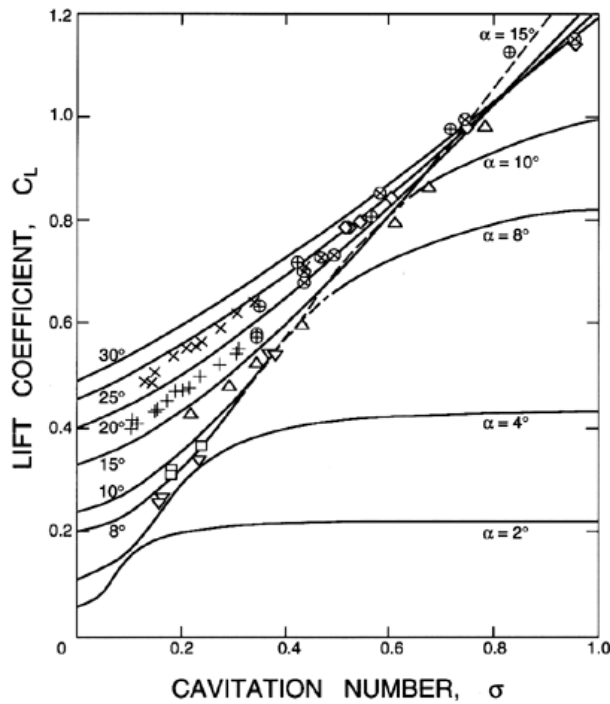
Figure 2: Lift coefficients for a flat plate from the nonlinear theory of Wu (1962). The experimental data (Parkin 1958) is for angles of incidence as follows: 8° (▽), 10° (□), 15° (△), 20° (⊕), 25° (⊗), and 30° (◇). Also shown is some data of Silberman (1959) in a free jet tunnel: 20° (+) and 25° (×).
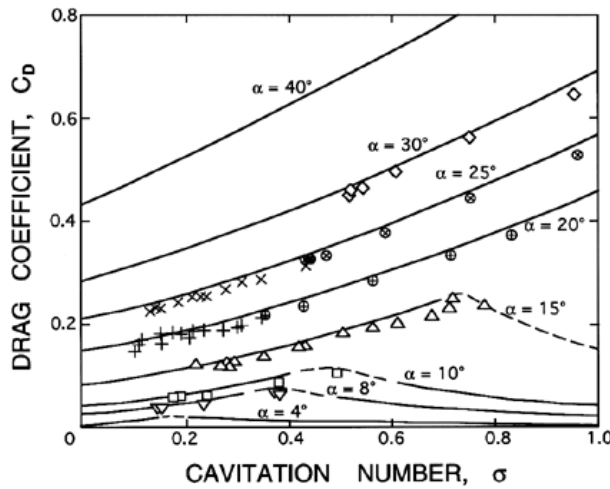

Figure 3: Drag coefficients corresponding to the lift coefficients of Figure 2.

where the value for $\sigma = 0$, namely $C_D = 0.88$, corresponds to the original solution of Kirchoff (in that case the cavity is infinitely long and the closure model is unnecessary). A good approximation to the form of equation (Nuf1) at low σ is

$$C_D(\sigma) = C_D(0)[1 + \sigma] \tag{Nuf2}$$

and it transpires that this is an accurate empirical formula for a wide range of body shapes, both planar and axisymmetric (see Brennen 1969a), provided the detachment is of the abrupt type. Bodies with smooth detachment such as a sphere (Brennen 1969a) are less accurately represented by equation (Nuf2) (see Figure 7).
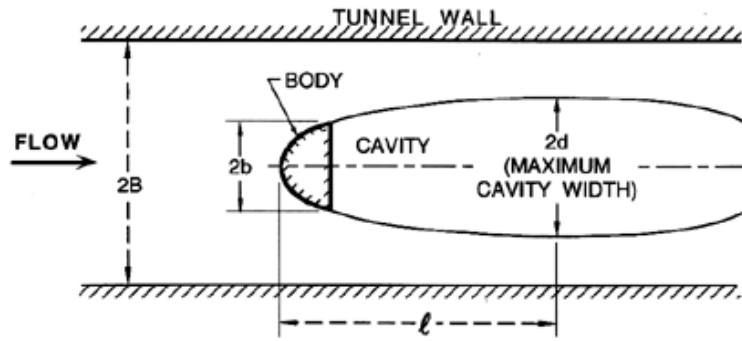
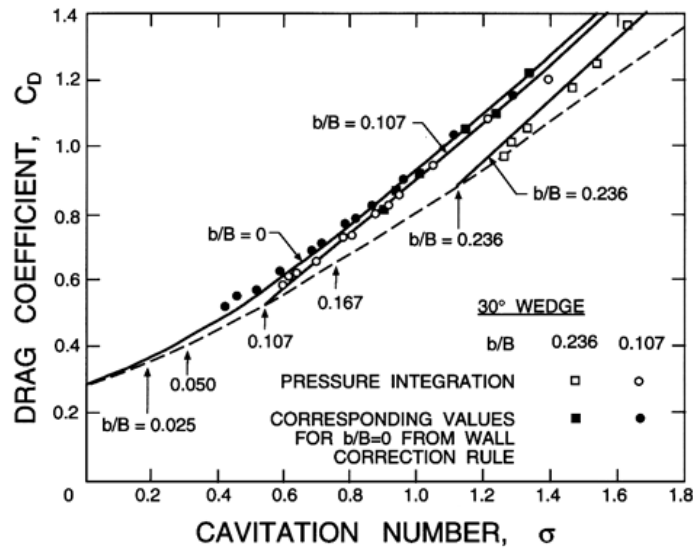Figure 4: Notation for planar flow in a water tunnel.

Figure 5: Analytical and experimental data for the drag coefficient, C_D, of a 30° half-angle wedge with a fully developed cavity in a water tunnel. Data are presented as a function of cavitation number, σ, for various ratios of wedge width to tunnel width, b/B (see Figure 4). Results are shown for the Riabouchinsky model (solid lines) including the choked flow conditions (dashed line with points for various b/B indicated by arrows), for the experimental measurements (open symbols), and for the experimental data corrected to $b/B \to 0$. Adapted from Wu, Whitney, and Brennen (1971).

Since experiments are almost always conducted in water tunnels of finite width, $2B$, another set of solutions of interest are those in which straight tunnel boundaries are added to the geometries of the preceding section, as shown in Figure 4. In the case of symmetric wedges in tunnels, solutions for the first three closure models of section (Nub) were obtained by Wu *et al.* (1971). Drag coefficients, cavity dimensions, and pressure distributions were computed as functions of cavitation number, σ, and blockage ratio, b/B. As illustrated in Figure 5, the results compare well with experimental measurements provided the cavitation number is low enough for a fully developed cavity to be formed. In the case shown in Figure 5, this cavitation number was about 1.5. The Riabouchinsky model results are shown in the figure since they were marginally better than those of the other two models insofar as the drag on the wedge was concerned. The variations with b/B are shown in Figure 5.

For comparative purposes, some results for a cavitating sphere in an axisymmetric water tunnel are presented in Figures 6 and 7. These results were obtained by Brennen (1969a) using a numerical method (see section (Nuk)). Note that the variations with tunnel blockage are qualitatively similar to those of planar flow. However, the calculated drag coefficients in Figure 7 are substantially larger than those
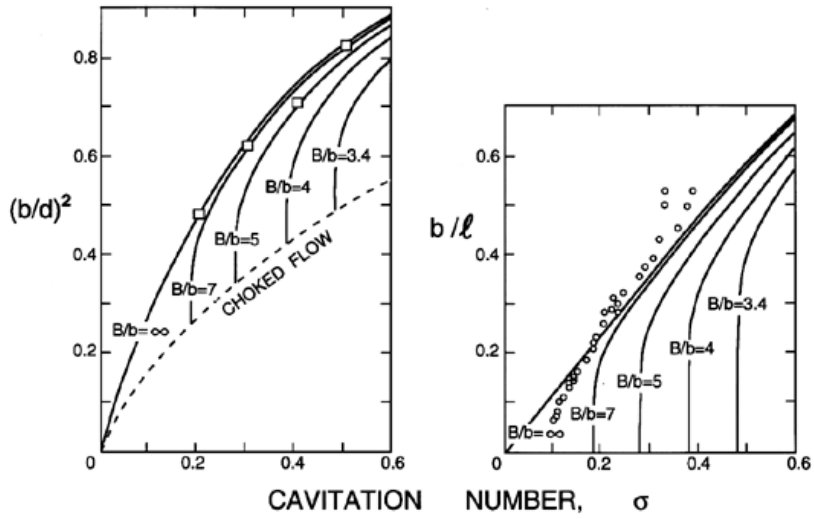
Figure 6: The dimensions of a fully developed cavity behind a sphere of radius, b, for various tunnel radii, B, from the numerical calculations of Brennen (1969a). On the left the maximum radius of the cavity, d, is compared with some results from Rouse and McNown (1948). On the right the half-length of the cavity, ℓ, is compared with the experimental data of Brennen (1969a) ($\circ$) for which $B/b = 14.7$.
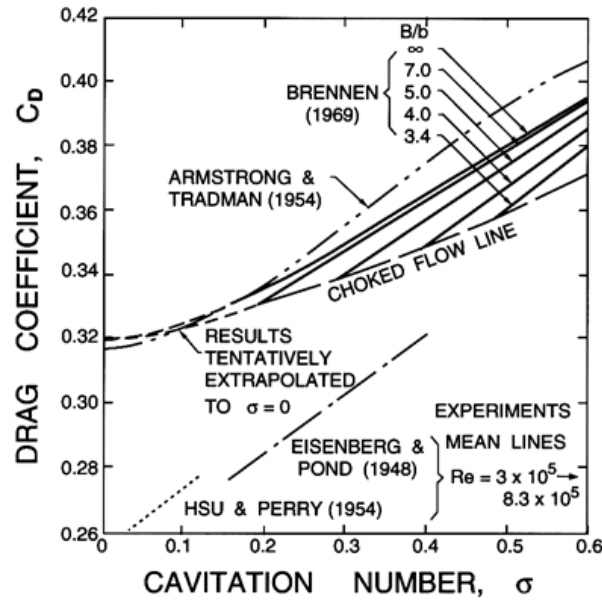

Figure 7: Calculated and measured drag coefficients for a sphere of radius, b, as a function of cavitation number, σ. The numerical results are by Armstrong and Tadman (1954) and Brennen (1969a) (for various tunnel radii, B) and the experimental data are from Eisenberg and Pond (1948) and Hsu and Perry (1954).

experimentally measured because of the difference in the detachment locations discussed in section (Nuc).

Reichardt (1945) carried out some of the earliest experimental investigations of fully developed cavities and observed that, when the cavitation number becomes very small, the maximum width, $2d$, and the length, 2ℓ, of the cavity in an unconfined flow ($b/B = 0$) vary roughly with σ in the following way:

- In planar flow:

$$d \propto \sigma^{-1} \quad ; \quad \ell \propto \sigma^{-2} \tag{Nuf3}$$

- In axisymmetric flow:

$$d \propto \sigma^{-\frac{1}{2}} \quad ; \quad \ell \propto \sigma^{-1} \tag{Nuf4}$$

The data for $b/B = 0$ in Figure 6 are crudely consistent with the relations of equation (Nuf4). Equations (Nuf3) and (Nuf4) provide a crude but useful guide to the relative dimensions of fully developed cavities at different cavitation numbers.